

Determination of primary microRNA processing in clinical samples by targeted pri-miR-sequencing

Thomas Conrad¹, Evgenia Ntini², Benjamin Lang³, Luca Cozzuto³, Jesper B Andersen⁴, Jens U
Marquardt⁵, Julia Ponomarenko^{3, 6}, Gian Gaetano Tartaglia^{3, 6}, Ulf A V Ørom^{7, *}

7 Affiliations:

8 1. Berlin Institute for Medical Systems Biology, Hannoversche Strasse 28, 10115 Berlin,
9 Germany

10 2. Max Planck Institute for Molecular Genetics, Ihnestrasse 63-73, 14195 Berlin, Germany

11 3. Centre for Genomic Regulation (CRG), The Barcelona Institute for Science and Technology,
12 C/ Dr. Aiguader 88, 08003 Barcelona, Spain

13 4. Biotech Research and Innovation Centre (BRIC), Department of Health and Medical Sciences,
14 University of Copenhagen, Ole Maaløes Vej 5, 2200 Copenhagen, Denmark

15 5. Universitätsklinikum Schleswig-Holstein, Ratzeburger Allee 160, 23538 Lübeck, Germany

16 6. University Pompeu Fabra (UPF), 08002 Barcelona, Spain

17 7. Aarhus University, Department of Molecular Biology and Genetics, C F MøllersAllé 3, 8000
18 Aarhus, Denmark

19 * Correspondence to: ulf.orom@mbg.au.dk (UAVØ)

22 **Abstract**

23 MicroRNA expression is important for gene regulation and deregulated microRNA expression is
24 often observed in disease such as cancer. The processing of primary microRNA transcripts is an
25 important regulatory step in microRNA biogenesis. Due to low expression level and association
26 with chromatin primary microRNAs are challenging to study in clinical samples where input
27 material is limited.

28 Here, we present a high-sensitivity targeted method to determine processing efficiency of several
29 hundred primary microRNAs from total RNA using as little as 500 thousand Illumina HiSeq
30 sequencing reads. We validate the method using RNA from HeLa cells and show the
31 applicability to clinical samples by analyzing RNA from normal liver and hepatocellular
32 carcinoma.

33 We identify 24 primary microRNAs with significant changes in processing efficiency from
34 normal liver to hepatocellular carcinoma, among those the highly expressed miRNA-122 and
35 miRNA-21, demonstrating that differential processing of primary microRNAs is occurring and
36 could be involved in disease. With our method presented here we provide means to study pri-
37 miRNA processing in disease from clinical samples.

38

39 **Key words:**

40 miRNA biogenesis, primary miRNAs, RNA sequencing, liver, HCC, clinical samples

41

42 **Introduction**

43 MicroRNAs (miRNA) are small RNAs that regulate gene expression at the post-transcriptional
44 level [1]. miRNAs are transcribed as primary miRNA (pri-miRNA) that can be several kilobases
45 long. These transcripts are processed in the nucleus to 60-90 nts long precursor miRNA hairpins
46 (pre-miRNA) by the Microprocessor complex. These pre-miRNAs are subsequently exported to
47 the cytoplasm by export factors where they are processed into 20-23 nts long mature miRNAs by
48 Dicer and incorporated into the RISC (RNA-induced silencing complex) to exert their regulatory
49 function [1].

50 We have previously showed that the endogenous Microprocessor activity toward individual pri-
51 miRNAs can be determined using RNA sequencing [2]. We identified a Microprocessor
52 cleavage signature and defined a metric for processing efficiency. We showed on a
53 transcriptome-wide scale that processing efficiency is highly variable among different canonical
54 pri-miRNAs and a major determinant of the expression levels of individual mature miRNAs. In
55 addition, we have showed that the kinetics of pri-miRNA processing vary between individual
56 transcripts, including within polycistronic transcripts [3].

57 *In vitro* assays looking at individual pri-miRNA transcripts have shown pri-miRNA processing
58 to be an actively regulated process that is responsive to TGF β signaling [4], DNA damage [5]
59 and cell density [6], and a recent study applied our pri-miRNA processing approach to
60 demonstrate that activation of the Type I interferon response in cells affects general pri-miRNA
61 processing [7]. Several Microprocessor co-factors have been identified that influence pri-miRNA
62 processing [2] and composition of the sequence flanking the pre-miRNA hairpin have been
63 shown to affect efficiency of Microprocessor cleavage [2, 8].

64 The major limitation of our approach to profile pri-miRNA processing transcriptome-wide has
65 been a requirement for purification of chromatin-associated RNA and large sequencing depth,
66 making analysis of clinical samples unfeasible. In the work reported here we aimed to improve
67 the approach to enable the analysis of pri-miRNA processing in clinical samples directly from
68 whole cell total RNA isolated from tissue. We used a targeted sequencing approach allowing for
69 quantification of 361 pri-miRNAs with as little as 500 thousand Illumina HiSeq reads, and
70 demonstrate the applicability to clinical samples using RNA from normal liver (NL) and
71 hepatocellular carcinoma (HCC) samples. We also identified differentially processed pri-
72 miRNAs between NL and HCC with a potential implication in disease.

73

74 **Results**

75 To determine pri-miRNA processing experimentally in clinical samples we expanded our RNA-
76 sequencing based methodology [2]. As mentioned above, the mature miRNA is generated in a
77 sequential manner starting with the transcription of a primary transcript [1]. The pre-miRNA is
78 cut out of the pri-miRNA by the Microprocessor complex (Figure 1a) consisting of Drosha and
79 DGCR8, in addition to a number of co-factors [9]. When using RNA-sequencing to high depth of
80 chromatin-associated RNA (enriching for pri-miRNA transcripts) a Microprocessor signature is
81 observed where the pre-miRNA has been cut out (Figure 1b) [2, 3]. This signature can be
82 quantified by determining the ratio between reads covering the pre-miRNAs and the flanking
83 sequence on the pri-miRNAs [2] (Supplementary Figure 1).

84 The major limitation of our published methodology is the requirement for enrichment of
85 chromatin-associated RNA and a high sequencing depth (for the development of the method we

86 used 200 million reads per sample). These requirements made the analysis of pri-miRNA
87 processing in total RNA from tissue and clinical samples unfeasible.
88 To overcome this limitation we developed a targeted approach to determine processing
89 efficiency of a library of selected pri-miRNAs from small amounts of starting material of total
90 RNA and low sequencing depth. We designed enrichment probes (xGEN lockdown probes,
91 Integrated DNA Technologies) covering the sequence of the pri-miRNA flanking the pre-
92 miRNA hairpin both upstream and downstream (Figure 2a). We targeted 32 pri-miRNAs that we
93 had already determined the processing efficiency for using chromatin-associated RNA and high
94 sequencing depth [2]. Each probe was designed to be complementary to the 120 nucleotides
95 immediately upstream or downstream of the Microprocessor cleavage sites, respectively. We
96 performed two independent enrichment experiments on RNA sequencing libraries generated
97 from chromatin-associated RNA to test the reproducibility of the enrichment approach (Figure
98 2b). We see a highly reproducible processing efficiency across all 32 pri-miRNAs for the two
99 samples ($R = 0.995$), demonstrating that the approach is robust and generates reproducible data.
100 We next asked how well the enrichment approach recapitulates the processing efficiencies
101 determined by high-depth sequencing without enrichment (Data from Conrad *et al.*, 2014). From
102 both independent probe enrichment replicates we see a high correlation ($R = 0.92$) in processing
103 efficiency when comparing to previous data of pri-miRNA processing from purified chromatin-
104 associated RNA (Figure 3a) [2]. Processing efficiencies and coverage for the 32 pri-miRNAs are
105 shown in Supplementary Table 1.
106 To assess the degree of enrichment achieved with the targeted approach we calculated RPKM
107 (Reads Per Kilobase per Million reads) for each of the 32 pri-miRNAs. As shown in Figure 3b
108 the enrichment is linear across the expression range of assayed pri-miRNAs ($R = 0.998$) with a

109 slope of 6,670-fold enrichment when using targeted sequencing of pri-miRNA transcripts. This
110 means that, in principle, 30,000 reads should be sufficient to determine processing efficiency for
111 selected pri-miRNAs when enriched from the chromatin fraction. Assuming that chromatin-
112 associated RNA constitutes 5 per cent of the total cellular (non-ribosomal) RNA 600,000 reads is
113 necessary to achieve robust determination of pri-miRNA processing from total RNA after
114 targeted enrichment.

115 To address differential pri-miRNA processing in clinical samples we used RNA from 40 HCC
116 tumors and 9 NL samples. We selected 361 miRNAs with a described involvement in cancer
117 [10–12] and designed 120-nts xGEN enrichment probes as illustrated in Figure 2a. For each
118 RNA sample we prepared a library for Illumina HiSeq 2500 sequencing and enriched with the
119 probe library as described in Materials and Methods. We aimed for 1 million reads per library
120 when multiplexing and the final output per library was between 500 thousand and 3 million
121 reads. With this sequencing depth we could detect the processing efficiency for 209 pri-miRNAs
122 in at least two samples, and show differential processing between HCC and NL for 24 of the pri-
123 miRNAs included in the analysis ($P < 0.05$, Wilcoxon rank test) (Figure 4a and Supplementary
124 Table 2). Of particular interest, we see the most statistically significant changes in the processing
125 of the liver-specific miR122 and the oncomiR miR21 (Figure 4b), where processing becomes
126 more efficient in HCC. In NL around 20 per cent of the pri-miRNA remains unprocessed
127 whereas in HCC there is an almost complete processing (a few per cent of the pri-miRNAs
128 remain unprocessed).

129

130

131

132 **Discussion**

133 We have previously shown that the processing efficiency of individual pri-miRNAs is similar
134 between three different cell lines (HeLa, HEK293 and A549), suggesting that diversity in
135 processing is largely dictated by the diverse substrate sequences. On the other side, several
136 studies have shown that co-factors and signaling pathways can regulate processing of individual
137 pri-miRNAs or groups of pri-miRNAs [4–8].

138 Here, we have developed a targeted version of our approach to measure endogenous pri-miRNA
139 processing for hundreds of different pri-miRNA at a time. Our targeted approach offers high
140 sensitivity to the selected pri-miRNAs and allows assessing numerous pri-miRNAs at a time in a
141 large collection of tissue and clinical samples. The method is particularly feasible to complement
142 total RNA sequencing studies as existing RNA sequencing libraries can directly be used for
143 targeted sequencing of pri-miRNA transcripts at very low cost once the enrichment probe library
144 has been designed.

145 We show that the targeted approach works well for clinical samples by demonstrating
146 reproducible differential processing of a number of pri-miRNAs between NL and HCC. Here, we
147 show that differential pri-miRNA processing occurs between NL and HCC suggesting that the
148 primary processing step in miRNA biogenesis can impact gene expression in disease. Our
149 targeted approach offers the possibility for further studies of pri-miRNA processing from clinical
150 samples that has so far not been feasible, allowing identification of the molecular consequences
151 of deregulated pri-miRNA processing in disease.

152

153 **Methods**

154 *Design of capture probes*

155 Capture probes were designed as xGEN Lockdown probes from IDT with the minimal
156 recommended length of 120 nts. For each pri-miRNA targeted by the library we made two
157 probes, one upstream and one downstream of the Microprocessor processing site.

158

159 *Enrichment of RNA sequencing library*

160 Targeted RNA sequencing libraries were enriched according to the xGEN guidelines with minor
161 modifications. In brief, 12 barcoded RNA sequencing libraries were pooled and 500 ng used for
162 each target enrichment. Blocking oligos were added to the pooled libraries, samples were dried
163 in a SpeedVac and resuspended in Hybridization buffer including the custom enrichment probes
164 and hybridized at 65 degrees for 4 hours after a 30 second incubation at 95 degrees. Streptavidin
165 beads were washed twice in Bead Wash Buffer before the capture reaction of custom enrichment
166 probes and targeted sequencing library. Samples were incubated 45 minutes at 65 degrees
167 followed by normal wash and two times high-stringency heated washes followed by an
168 additional wash at room temperature and elution of captured library with nuclease-free water.
169 The captured libraries were amplified with PCR using KAPA HiFi Hotstart polymerase for 14
170 cycles. The post-capture PCR fragment were purified with Agencourt AMPure XP beads before
171 sequencing of the targeted libraries.

172

173 *Data analysis and calculation of processing efficiency*

174 Raw reads were inspected for quality using FastQC (v0.11.5). Reads were then trimmed with
175 skewer (version 0.2.2) for removing the adapters and low quality reads. Processed reads were

176 aligned to the reference genome (human, GENCODE release 27, GRCh38.p10) using STAR
177 aligner (version 2.5.3a). bedtools "genomecov" was run on the aligned reads with the "-split"
178 option for calculating the coverage. The coverage was multiplied for a scaling factor (using the
179 parameter "-scale") that is obtained by dividing 1 billion / (number of mapped reads * read size).
180 The BED graph was converted to bigWig using bedGraphToBigWig. Custom scripts were used
181 to calculate read count averages and the processing efficiency was calculated by counting the
182 reads covering the pre-miRNA region divided by the reads covering the two 100 nts flanking
183 regions of the pri-miRNA (starting 20 nts from the stem to avoid noise in read coverage), and
184 normalized to the length of each pri-miRNA in nts (Supplementary Figure 1). Pre-miRNAs were
185 annotated from the sequence of the mature miRNAs so that each pre-miRNA starts with the first
186 base of the 5P miRNA and ends with the last base of the 3P miRNA.

187

188 *Data availability*

189 All sequencing data have been deposited to GEO under accession number GSE148756 and
190 GSE149631.

191

192 **Author contributions**

193 Conceived experiments: TC, UAVØ; Performed experiments: TC, UAVØ; Analyzed data: EN,
194 BL, LC; Contributed clinical samples: JBA, JM; Supervised computational work: EN, JP, GGT;
195 Supervised experimental work: UAVØ; Interpreted data: TC, EN, BL, LC, JP, GGT, UAVØ;
196 Secured funding: UAVØ; Wrote the manuscript: TC, BL, UAVØ; Commented on the manuscript
197 and approved the final version: All authors.

198

199 **Acknowledgments**

200 This work was funded by the Sofja Kovalevskaja Award of the Alexander von Humboldt
201 Foundation and the Hallas Møller Award of the Novo Nordisk Foundation (UAVØ).

202

203 **Figure legends**

204

205 **Figure 1. The Microprocessor signature**

206 (a) The general structure of a pri-miRNA with the hairpin pre-miRNA and the Microprocessor
207 cleavage site indicated. (b) Example of the Microprocessor signature around the pre-miRNA in
208 an RNA sequencing read density plot.

209

210 **Figure 2. Enrichment of pri-miRNAs for determination of processing efficiency**

211 (a) Schematic of a pri-miRNA and the localization of our enrichment probes. (b) Reproducibility
212 of processing efficiency for 32 pri-miRNAs between two independent replicates from RNA
213 sequencing libraries generated from chromatin-associated RNA.

214

215 **Figure 3. Reproducibility and sensitivity of pri-miRNA processing efficiency determination**

216 (a) Correlation of processing efficiency determined from high-depth sequencing of chromatin-
217 associated RNA [2] and low-depth sequencing of targeted sequencing of total RNA for two
218 technical replicates. (b) Sensitivity of each approach determined by RPKM at pri-miRNAs.
219 Slope shows a 6,670-fold increase in sensitivity and a corresponding decreased need for
220 sequencing depth. RPKM for targeted sequencing is calculated as the average of two
221 independent enrichment replicates.

222

223 **Figure 4. Differential pri-miRNA processing between NL and HCC**

224 (a) Heat-map of pri-miRNA levels of the 24 differentially processed pri-miRNAs between HCC
225 and NL. (b) Increased processing of pri-miRNAs in HCC compared to NL for miR-122 and miR-
226 21. Shown is the pri-miRNA level as the proportion of the pri-miRNA that remains unprocessed
227 as determined by RNA sequencing. *** p < 0.0001, Wilcoxon rank test.

228

229

230

231

232

233

234

235

236

237

238

239

240

241

242

243

244

245 **References**

246 1. Kim VN, Han J, Siomi MC (2009) Biogenesis of small RNAs in animals. *Nat. Rev. Mol.*
247 *Cell Biol.*

248 2. Conrad T, Marsico A, Gehre M, Ørom UA (2014) Microprocessor activity controls
249 differential miRNA biogenesis in vivo. *Cell Rep.*
250 <https://doi.org/10.1016/j.celrep.2014.09.007>

251 3. Louloupi A, Ntini E, Liz J, Ørom UA (2017) Microprocessor dynamics shows co- and
252 post-transcriptional processing of pri-miRNAs. *RNA.*
253 <https://doi.org/10.1261/rna.060715.117>

254 4. Davis BN, Hilyard AC, Lagna G, Hata A (2008) SMAD proteins control DROSHA-
255 mediated microRNA maturation. *Nature.* <https://doi.org/10.1038/nature07086>

256 5. Suzuki HI, Yamagata K, Sugimoto K, et al (2009) Modulation of microRNA processing
257 by p53. *Nature.* <https://doi.org/10.1038/nature08199>

258 6. Mori M, Triboulet R, Mohseni M, et al (2014) Hippo signaling regulates microprocessor
259 and links cell-density-dependent mirna biogenesis to cancer. *Cell.*
260 <https://doi.org/10.1016/j.cell.2013.12.043>

261 7. Witteveldt J, Ivens A, Macias S (2018) Inhibition of Microprocessor Function during the
262 Activation of the Type I Interferon Response. *Cell Rep.*
263 <https://doi.org/10.1016/j.celrep.2018.05.049>

264 8. Auyeung VC, Ulitsky I, McGahey SE, Bartel DP (2013) Beyond secondary structure:
265 Primary-sequence determinants license Pri-miRNA hairpins for processing. *Cell.*
266 <https://doi.org/10.1016/j.cell.2013.01.031>

267 9. Gregory RI, Yan KP, Amuthan G, et al (2004) The Microprocessor complex mediates the

268 genesis of microRNAs. *Nature*. <https://doi.org/10.1038/nature03120>

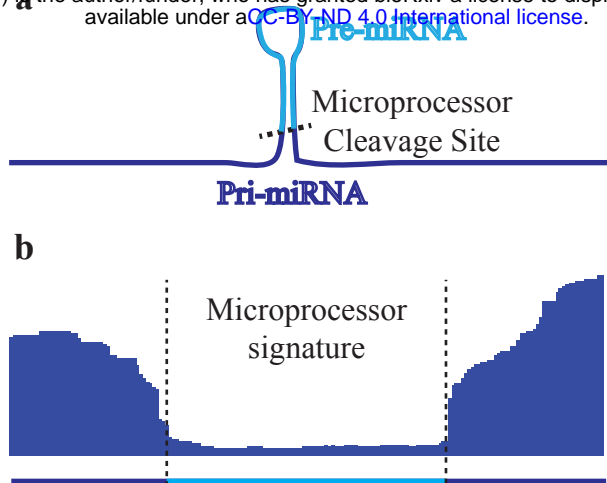
269 10. Volinia S, Galasso M, Sana ME, et al (2012) Breast cancer signatures for invasiveness and
270 prognosis defined by deep sequencing of microRNA. *Proc Natl Acad Sci U S A*.
271 <https://doi.org/10.1073/pnas.1200010109>

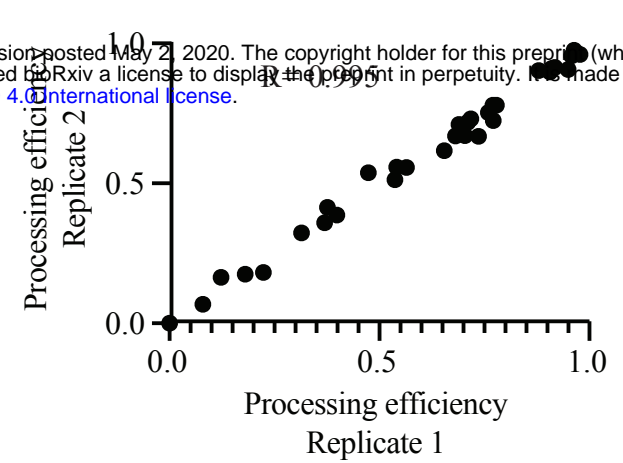
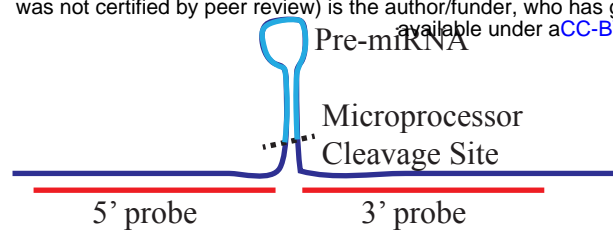
272 11. Wong NW, Chen Y, Chen S, Wang X (2018) OncomiR: An online resource for exploring
273 pan-cancer microRNA dysregulation. *Bioinformatics*.
274 <https://doi.org/10.1093/bioinformatics/btx627>

275 12. Farazi TA, Horlings HM, Ten Hoeve JJ, et al (2011) MicroRNA sequence and expression
276 analysis in breast tumors by deep sequencing. *Cancer Res*. <https://doi.org/10.1158/0008-5472.CAN-11-0608>

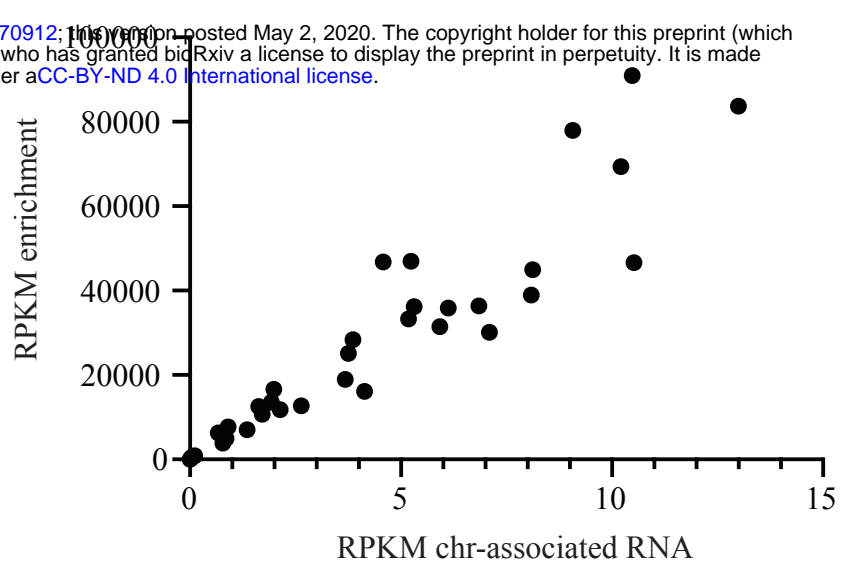
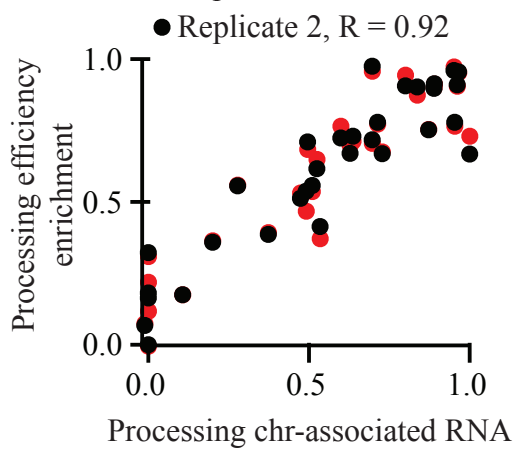
278

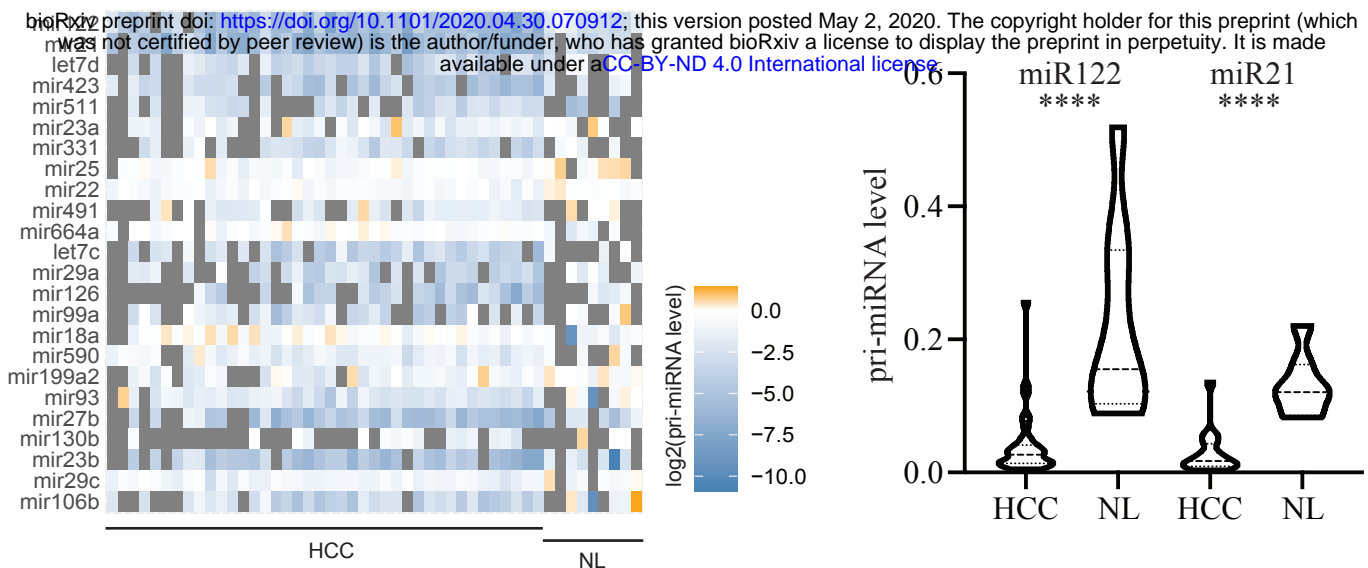
279





a bioRxiv preprint doi: <https://doi.org/10.1101/2020.04.30.207012>; this version posted May 2, 2020. The copyright holder for this preprint (which was not certified by peer review) is the author/funder, who has granted bioRxiv a license to display the preprint in perpetuity. It is made available under aCC-BY-ND 4.0 International license.



a**b**